

PARTICLE TRANSPORT IN TANGLED MAGNETIC FIELDS AND FERMI ACCELERATION AT RELATIVISTIC SHOCKS

MARTIN LEMOINE¹

GReCO / Institut d'Astrophysique de Paris, CNRS,
98 bis boulevard Arago, F-75014 Paris, France

GUY PELLETIER²

Laboratoire d'Astrophysique de Grenoble LAOG,
CNRS, Université Joseph Fourier,
BP 53, F-38041 Grenoble, France,
Institut Universitaire de France
Draft version March 20, 2019

ABSTRACT

This paper presents a new method of Monte-Carlo simulations of test particle Fermi acceleration at relativistic shocks. The particle trajectories in tangled magnetic fields are integrated out exactly from entry to exit through the shock, and the conditional probability of return as a function of ingress and egress pitch angles is constructed by Monte-Carlo iteration. These upstream and downstream probability laws are then used in conjunction with the energy gain formula at shock crossing to reproduce Fermi acceleration. For pure Kolmogorov magnetic turbulence upstream and downstream, the spectral index is found to evolve smoothly from $s = 2.09 \pm 0.02$ for mildly relativistic shocks with Lorentz factor $\Gamma_s = 2$ to $s \simeq 2.26 \pm 0.04$ in the ultra-relativistic limit $\Gamma_s \gg 1$. The energy gain is $\sim \Gamma_s^2$ at first shock crossing, and ~ 2 in all subsequent cycles as anticipated by Gallant & Achterberg (1999). The acceleration timescale is found to be as short as a fraction of Larmor time when $\Gamma_s \gg 1$.

Subject headings: shock waves – acceleration of particles – cosmic rays

1. INTRODUCTION

Fermi acceleration at relativistic shocks is an important topic for understanding the formation of spectra of ultrarelativistic particles and radiation in relativistic flows such as those observed in active nuclei, microquasars, γ -ray bursts and pulsar wind nebulae (see Kirk & Duffy 2001 and references therein). Of particular interest is the acceleration timescale that can be as short as a Larmor time for relativistic Fermi acceleration; the smaller return probability to the shock for downstream particles, as compared to the non-relativistic regime, is compensated by the much larger energy gain at each cycle. However the study of Fermi acceleration in the relativistic limit is more involved than in the non-relativistic regime due to the increased importance of the anisotropy of the distribution function (Gallant & Achterberg 1999).

Various methods have been used to study the relativistic regime of Fermi acceleration (see Kirk & Duffy 2001 and references therein), starting with analytical estimates by Peacock (1981), followed by semi-analytical methods (Kirk & Schneider 1987; Gallant & Achterberg 1999; Kirk et al. 2000; Achterberg et al. 2001) and numerical Monte-Carlo techniques (Ballard & Heavens 1992; Ostrowski 1993; Bednarz & Ostrowski 1998), which in spite of their differences converge to an asymptotic spectral index $s \approx 2.2 - 2.3$ in the ultra-relativistic limit.

In the present *Letter*, we propose a new numerical Monte-Carlo method of simulation of the acceleration of test particles at relativistic shocks. The trajectories of particles in the upstream and downstream inhomogeneous magnetic fields are integrated out exactly from the entry of each particle through the shock until its first return to the shock. The law of probability of return to the shock as a function of ingress and egress pitch

angles is then constructed by Monte-Carlo iteration. Finally we combine these probability laws, one defined for upstream and the other for downstream, with the energy gain formula at shock crossing to simulate the acceleration process. This latter use of the angular probability laws is similar to the method of Gallant et al. (2000) with some differences to be discussed below.

The present method appears efficient and potentially more powerful when compared to direct Monte-Carlo simulations which follow each particle through its repeated shock crossings (e.g. Ballard & Heavens 1992; Ostrowski 1993). It allows one to simulate relativistic Fermi acceleration in any magnetic configuration, albeit for test particles only. We describe the method and numerical simulations in Section 2 and then present the results for a planar shock with fully turbulent magnetic field both upstream and downstream in Section 3.

2. NUMERICAL SIMULATIONS

The hydrodynamic jump conditions at an adiabatic strong shock, neglecting magnetic fields, are given in Blandford & Mc Kee (1977), Kirk & Duffy (2001) and Gallant (2002). The shock Lorentz factor is Γ_s (upstream or lab frame³), and the relative Lorentz factor Γ_r between upstream and downstream $\Gamma_r \equiv \Gamma_s \Gamma_{s|d} (1 - \beta_s \beta_{s|d})$. The downstream Lorentz factor $\Gamma_{s|d}$ (and Γ_r) can be obtained as a function of Γ_s from the relations derived from the shock jump conditions given in Gallant (2002). In particular, in the ultra-relativistic limit $\Gamma_s \rightarrow +\infty$, one finds the well-known results $\beta_{s|d} \rightarrow 1/3$ and $\Gamma_r \rightarrow \Gamma_s/\sqrt{2}$.

We conduct our simulations in two steps. We first perform Monte-Carlo simulations of particle propagation in a given magnetic field structure following Casse, Lemoine & Pelletier

¹ email: lemoine@iap.fr

² email: guy.pelletier@obs.ujf-grenoble.fr

³ Unless otherwise noted, all quantities are calculated in the upstream (lab) frame; wherever needed, quantities relative to a given frame but calculated in an other will be marked with the subscript |, e.g., $\beta_{s|d}$ refers to the shock velocity measured in the downstream rest frame.

(2001) (wherein one may find more details on the numerical procedure). These simulations are carried out separately in the downstream and in the upstream rest frames. It is possible to set up any magnetic field structure including regular and tangled components, but in the following, for the sake of simplicity, we restrict ourselves to the case of pure Kolmogorov turbulence in both downstream and upstream rest frames. The equations of motion of each particle are integrated out exactly, the magnetic field being calculated at each point of the trajectory as a sum of plane waves, using 200 modes spaced logarithmically on three decades of wavelength and whose wavevector directions are drawn at random⁴. Ostrowski (1993) used a similar technique to construct the magnetic field albeit with 3 modes only, while Ballard & Heavens (1992) used three-dimensional FFT methods (see Casse, Lemoine & Pelletier 2001 for a comparison of these methods).

The trajectories are integrated over 100 scattering times upstream and 1000 scattering times downstream in order not to miss possible late returns to the shocks. The laws of return probability as a function of ingress and egress pitch angles are then constructed in the following way. We draw at random a point along a simulated trajectory which defines the point of entry through the shock. The ingress pitch angle cosine to shock normal μ^i is recorded, the trajectory scanned to find the point of exit through the shock, and the egress pitch angle cosine μ^e is then recorded. Iteration of the above then yields the desired law of conditional return probability $\mathcal{P}(\mu^i; \mu^e)$ which gives the probability for a particle entering with a pitch angle cosine μ^i to return to the shock with a pitch angle cosine μ^e . The simulations also give a direct measurement of the return time to the shock as a function of pitch angles.

Once the upstream and downstream laws of return probability, respectively $\mathcal{P}_u(\mu_u^i; \mu_u^e)$ and $\mathcal{P}_d(\mu_d^i; \mu_d^e)$ are known, the simulation of the acceleration process itself can be performed as follows. We denote by $f_d^{2n+1}(\mu_d, \epsilon_d)$ the distribution function of particles that enter the shock to downstream and that have experienced $2n+1$ shock crossings, and $f_u^{2n}(\mu_u, \epsilon_u)$ similarly upstream: particles are upstream for an even number of shock crossings and f_u^0 represents the injection population. These distribution functions are normalized to the total number of particles N injected such that, in the absence of escape from the acceleration site, after $2n$ shock crossings $N = \int d\mu_u d\epsilon_u f_u^{2n}(\mu_u, \epsilon_u)$, and after $2n+1$ shock crossings $N = \int d\mu_d d\epsilon_d f_d^{2n+1}(\mu_d, \epsilon_d)$. The conservation of particle number at shock crossing $u \rightarrow d$ and Lorentz transforms of pitch angles and energies imply:

$$f_d^{2n+1}(\epsilon_d, \mu_d^i) d\mu_d^i d\epsilon_d = \left[\int_{\beta_s}^1 d\mu_u^i \mathcal{P}_u(\mu_u^i; \mu_u^e) f_u^{2n}(\epsilon_u; \mu_u^i) \right] d\mu_u^e d\epsilon_u \quad (1)$$

$$\mu_d^i = \frac{\mu_u^e - \beta_r}{1 - \beta_r \mu_u^e}, \quad \epsilon_d = \Gamma_r (1 - \beta_r \mu_u^e) \epsilon_u, \quad (2)$$

and one obtains a similar system for shock crossing $d \rightarrow u$:

$$f_u^{2n}(\epsilon_u, \mu_u^i) d\mu_u^i d\epsilon_u = \left[\int_{-1}^{\beta_{s|d}} d\tilde{\mu}_d^i \mathcal{P}_d(\tilde{\mu}_d^i; \mu_d^e) f_d^{2n-1}(\tilde{\epsilon}_d; \tilde{\mu}_d^i) \right] d\mu_d^e d\tilde{\epsilon}_d \quad (3)$$

$$\mu_u^i = \frac{\mu_d^e + \beta_r}{1 + \beta_r \mu_d^e}, \quad \epsilon_u = \Gamma_r (1 + \beta_r \mu_d^e) \tilde{\epsilon}_d, \quad (4)$$

The terms within brackets in Eqs. (1) and (3) correspond to the distribution function upon exit from upstream and downstream respectively. The return probability to the shock $P_{\text{ret}}(\mu_d^i)$ as a function of ingress pitch angle can be obtained as: $P_{\text{ret}}(\mu_d^i) \equiv \int d\mu_d^e \mathcal{P}_d(\mu_d^i; \mu_d^e)$. The corresponding return probability for upstream is obviously unity. After each cycle $u \rightarrow d \rightarrow u$, a fraction $f_{\text{out}}^{2n+1}(\epsilon) = \int d\mu_d^i [1 - P_{\text{ret}}(\mu_d^i)] f_d^{2n+1}(\mu_d^i; \epsilon)$ of the particle population has escaped downstream and accumulates to form the outgoing particle population $f_{\text{out}}(\epsilon) = \sum_{n=0}^{+\infty} f_{\text{out}}^{2n+1}(\epsilon)$. By following each shock crossing, and using Eqs. (1),(2),(3), (4) one can follow the evolution of f_d , f_u and f_{out} , starting from a mono-energetic and isotropic initial injection distribution upstream. The distribution $f_{\text{out}}(\epsilon)$ eventually provides the accelerated particle population. A similar formal development of the acceleration process by repeated shock crossings has been proposed independently by Vietri (2002): the flux of particles crossing the shock in the stationary regime, noted J_{in} in Vietri (2002) is related to the above as $J_{\text{in}} = C \sum_{n=0}^{+\infty} f_d^{2n+1}$ with C a normalization constant.

This method assumes that the angular probability laws do not depend on rigidity. This is true in the diffusive limit but one might expect some weak dependence to appear in the relativistic limit $\Gamma_s \gg 1$. Indeed we have found numerically such a weak dependence of \mathcal{P}_d and \mathcal{P}_u on the particle rigidity. However it remains weak, and the change in \mathcal{P} averages to a few percent when the rigidity changes by two orders of magnitude. In terms of energy spectral index s , this dependence introduces an error of $\delta s = \pm 0.02$ for $\Gamma_s = 2$ up to $\delta s = \pm 0.04$ for $\Gamma_s = 100$. Therefore in the following we neglect the dependence on rigidity but keep the above errors as uncertainties on our results. Note that one can in principle incorporate this dependence on rigidity in our method at the expense of having to calculate the probability laws \mathcal{P} for a wide range of values of the rigidity.

The present technique has significant advantages when compared to standard Monte-Carlo techniques which follow the particle trajectories on both sides of the shock through the whole acceleration process. Indeed, provided one neglects the dependence on rigidity of \mathcal{P} , one can simulate the trajectories of particles of high rigidity only (near the end of the resonance range) which are must faster to integrate than the trajectories of particles of small rigidity since the ratio of scattering time to Larmor time decreases with increasing rigidity. The direct Monte-Carlo methods also suffer from the problem of a small dynamic range of the magnetic fields as compared to the wide dynamic range of particles momenta. The present method also offers a significant gain in signal as will be obvious in the following. Finally our method differs from Gallant et al. (2000) as they use Itô differential techniques to simulate scattering downstream and analytical methods for scattering in a regular magnetic field upstream assuming $\Gamma_s \gg 1$. In contrast, the present simulations can be applied to any shock Lorentz factor and magnetic field configuration. Furthermore they use Monte-Carlo methods to simulate the acceleration process after constructing the laws of return probability while we directly fold over repeatedly the probability distributions in conjunction with the energy gain formula.

3. RESULTS

The downstream return probability to the shock as a function of ingress pitch angle cosine is shown in Fig. 1 for $\Gamma_s = 2, 100$.

⁴ Using a higher number of modes does not modify the results shown here as we have checked.

The return probability for $\Gamma_s = 100$ is an asymptote which is reached to within a percent as early as $\Gamma_s = 5$. In Fig. 2, we show the average energy gain $\langle g \rangle \equiv \langle \epsilon_f \rangle / \langle \epsilon_i \rangle$ per cycle $u \rightarrow d \rightarrow u$ (diamonds) and $d \rightarrow u \rightarrow d$ (triangles) for $\Gamma_s = 100$. This energy gain is defined as the ratio of the average energies at the end (ϵ_f) and at the beginning of the cycle (ϵ_i), with $\langle \epsilon \rangle \equiv \int d\mu d\epsilon \epsilon f(\mu, \epsilon) / \int d\mu d\epsilon f(\mu, \epsilon)$. The average energy gain in each cycle subsequent to first shock crossing is $\simeq 1.93$ per cycle $u-d-u$ for $\Gamma_s = 100$, and this asymptotic value is reached immediately after the first cycle. This is a rather dramatic confirmation of the analytical expectations of Gallant & Achterberg (1999) and Achterberg et al. (2001) which had argued that only the first cycle should yield a gain $\approx \Gamma_s^2$ since the anisotropy of the distribution function upstream is so pronounced that the gain in subsequent cycles is reduced to ≈ 2 .

An example of the spectrum of accelerated particles for $\Gamma_s = 100$ after 20 cycles $u \rightarrow d \rightarrow u$ is shown in Fig. 3; the thin lines in this figure show the fractions of particles f_{out}^{2n+1} that escape after $2n+1$ shock crossings. One clearly sees in this figure the piling up of populations of particles of ever decreasing size (due to finite escape probability) and ever increasing energy which gives rise to the accelerated population $f_{\text{out}} = \sum_n f_{\text{out}}^{2n+1}$. The spectral index of the escaping population for $\Gamma_s = 100$ is here $s = 2.26 \pm 0.04$ (incorporating the error due to dependence of \mathcal{P} on rigidity), in excellent agreement with previous results by Bednarz & Ostrowski (1998), Kirk et al. (2000) and Achterberg et al. (2001).

Finally, in Fig. 4, we give the average return probabilities (open squares), average asymptotic energy gains (diamonds) and spectral indices (filled circles) for values of Γ_s comprised between 2 and 100. The average return probabilities shown in this figure are the return probabilities shown in Fig. 1 weighted by the corresponding asymptotic downstream ingress pitch angle distribution, i.e. $\langle P_{\text{ret}} \rangle = \lim_{n \rightarrow +\infty} \int \mathcal{P}_{\text{ret}}(\mu_d^i) f_d^n(\mu_d^i) d\mu_d^i / \int f_d^n(\mu_d^i) d\mu_d^i$. A naive unweighted average of the return probability shown in Fig. 1 for $\Gamma_s = 100$ would give 0.33, whereas the weighted average gives 0.40: the difference is directly related to the strong anisotropy at shock crossing.

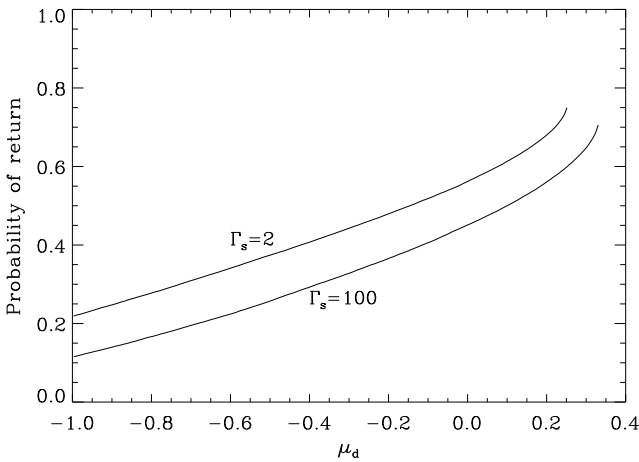


FIG. 1.— Probability of return to shock $P_{\text{ret}}(\mu_d)$ downstream as a function of ingress downstream pitch angle cosine μ_d for $\Gamma_s = 2, 100$. Note that the probability is defined for $-1 \leq \mu_d \leq \beta_{s|d}$ due to shock crossing conditions on μ_d .

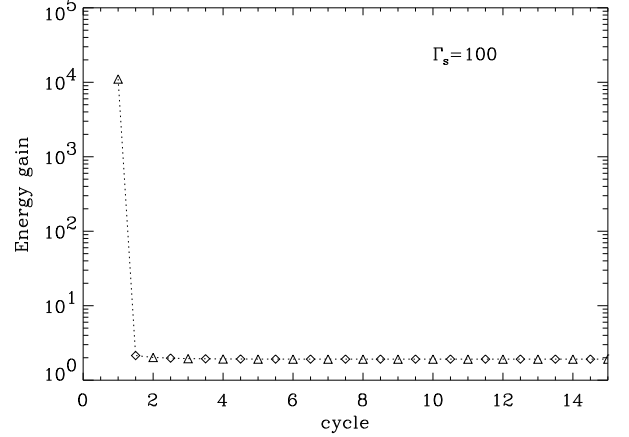


FIG. 2.— Averaged energy gain per cycle $u \rightarrow d \rightarrow u$ (diamonds) and $d \rightarrow u \rightarrow d$ (triangles) for $\Gamma_s = 100$.

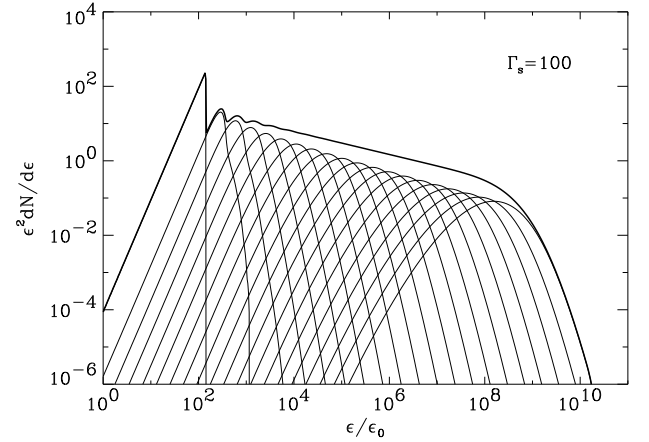


FIG. 3.— Spectrum of particles escaping downstream (thick line) as a function of momentum after 20 cycles for $\Gamma_s = 100$; in thin lines, the spectra of particles escaping downstream after each cycle.

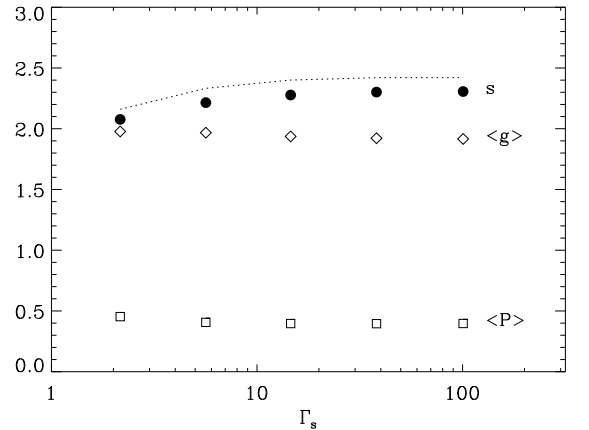


FIG. 4.— Average return probabilities (open squares), average energy gain per cycle (dopen diamonds) and spectral slope (filled circles) as a function of Γ_s . The dotted line shows the approximation to the spectral slope given by the Bell formula using the average return probabilities and energy gains (see text).

The standard non-relativistic formula for the (energy) spectral index s (Bell 1978), $s = 1 - \log(\langle P_{\text{ret}} \rangle) / \log(\langle g \rangle)$, with $\langle g \rangle$ the average energy gain, is in relatively good agreement with

the slopes obtained, provided one uses the weighted average for the return probability as above, see Fig. 4. A more general formula which includes relativistic effects has been proposed by Vietri (2002): $\langle P_{\text{ret}} \rangle \langle g^{s-1} \rangle = 1$. One can derive this formula and variants of it by using our Eqs. (1),(2),(3), (4). For instance, insert Eq. (3) into Eq. (1) then sum over n (shock crossing number) to go to the stationary regime and consider an energy range where $\epsilon \gg \epsilon_0$, ϵ_0 being the maximal injection energy. There one expects that $\sum_n f_d^{2n+1} \propto \epsilon_d^{-s} \phi(\mu_d)$, i.e. the distribution factorizes out in an energy power law times a function of pitch angle, and indeed this property is verified numerically to high accuracy. Then one introduces the energy gain per cycle $g(\mu_d^c, \mu_d^i) = \epsilon_d / \bar{\epsilon}_d$ and integrates over μ_d^i both sides of the equation. Finally, dividing one side by the other yields the following relation, which is a variant of the formula of Vietri (2002):

$$\int_{-1}^{\beta_{s|d}} d\mu_d^i \int_{\beta_{s|d}}^1 d\mu_d^c \bar{P}_{\text{ret}}(\mu_d^c) \bar{P}_u(\mu_d^c, \mu_d^i) g^{s-1}(\mu_d^c, \mu_d^i) = 1. \quad (5)$$

In this equation, $\bar{P}_u(\mu_d^c, \mu_d^i)$ simply corresponds to \mathcal{P}_u expressed in terms of downstream pitch angle cosines, and $\bar{P}_{\text{ret}}(\mu_d^c) \equiv \int d\mu_d^i \mathcal{P}_d(\mu_d^i, \mu_d^c)$. Equation (5) is indeed verified to within the numerical noise ($< 1\%$).

Our simulations also provide a direct measurement of the acceleration timescale, which can be defined as the cycle time in the upstream rest frame when $\Gamma_s \gg 1$: $t_{\text{acc}}(\epsilon) \approx t_{u|u}(\epsilon) + \Gamma_r t_{d|d}(\epsilon / \Gamma_r)$, where $t_{u|u}(\epsilon)$ and $t_{d|d}(\epsilon)$ denote the upstream and downstream return times measured in their respective rest frames for a particle of energy ϵ . For $t_{d|d}$ we find to within the noise of the simulations: $t_{d|d} \simeq 1.5 \beta_{s|d}^{-1} t_{\text{scatt}|d}$, with $t_{\text{scatt}|d}$ the scattering time downstream. The scattering time is given as a function of Larmor time t_L in Casse, Lemoine & Pelletier (2001), and for pure turbulence one finds: $t_{\text{scatt}}/t_L \simeq 0.4 \rho^{-2/3}$ for $\rho \lesssim 0.1$ and $t_{\text{scatt}}/t_L \simeq 2$ for $0.1 \lesssim \rho \lesssim 1$. Here $\rho \equiv k_{\text{min}} r_L$ denotes the rigidity, with k_{min} the smallest wavenumber of the magnetic field modes. The above result for $t_{d|d}$ can be understood as follows. In the non-relativistic limit one derives $t_{d|d} \simeq (2/3 \beta_{s|d}^2) (1 - \langle P_{\text{ret}} \rangle) / \langle P_{\text{ret}} \rangle$ and we find $\langle P_{\text{ret}} \rangle \sim (1 - \beta_{s|d})/2$ in the relativistic limit, which gives $t_{d|d} \sim t_{\text{scatt}|d} / \beta_{s|d}$.

Gallant & Achterberg (1999) have conjectured $t_{u|u} \approx t_{L|u} / \Gamma_s$

for $\Gamma_s \gg 1$, corresponding to deflection by an angle of order $1/\Gamma_s$ in a regular magnetic field. We confirm this result up to a small residual dependence on scattering time/rigidity: $t_{u|u} \approx 5 \Gamma_s^{-1} \rho_u^{-0.15} t_{L|u}$ for $\Gamma_s \gtrsim 5$. In the mildly relativistic case, for $\Gamma_s = 2$, we find $t_{u|u} \approx t_{\text{scatt}|u}$, which indicates that the particles have time to wander before being caught by the shock in this case.

The final acceleration time depends on how the magnetic field downstream B_d is related to that upstream B_u (Gallant & Achterberg 1999). If one assumes that $B_d = \Gamma_B B_u$ with $\Gamma_B \sim \Gamma_s$, and the turbulence is isotropic downstream but the length scale has been contracted by a factor $\sim \Gamma_B$, i.e. $k_{\text{min}|d} \sim \Gamma_B k_{\text{min}|u}$, one finds, for $\rho_{d|d} \simeq 1$, $t_{\text{acc}} \sim (5 \Gamma_s^{-0.15} + 9) t_{L|u} / \Gamma_s$. The acceleration timescale can thus be as short as a fraction of Larmor time in the ultra-relativistic limit.

This is a most interesting aspect of relativistic Fermi acceleration, as it implies that the particles can reach the energy confinement limit $\epsilon_{\text{cl}} = Ze \Gamma_B r$ when the acceleration is limited by expansion losses or by the age of the shock wave. Here, $r = \min(l, t/\kappa c)$, l is the size of the accelerating region, t the age or losses timescale and $\kappa = t_{\text{acc}}/t_L < 1$, all quantities being expressed in the comoving frame. This is particularly relevant for the generation of ultra-high energy cosmic rays in relativistic winds such as γ -ray bursts (Waxman 1995, Vietri 1995, Gallant & Achterberg 1999, Gialis & Pelletier 2003). In particular our results for $\Gamma_s = 2$ are of direct relevance to the acceleration of protons and electrons in internal shocks of γ -ray bursts, while the results for $\Gamma_s \gg 1$ can be applied directly to the external shock model of γ -ray bursts.

To sum up, our simulations confirm the results of Bednarz & Ostrowski (1998) concerning the spectral index and those of Achterberg et al. (2001) concerning the spectral index, the acceleration time scale and energy gains. Very recently, Ellison & Double (2002) found a similar index by taking into account the backreaction of cosmic rays on the shock structure. In the near future, the present method will be applied to more general magnetic field configurations including parallel, transverse, subluminal and superluminal shocks.

We would like to thank Y. Gallant for fruitful discussions.

REFERENCES

- Achterberg, A., Gallant, Y. A., Kirk, J. G., & Guthmann, A. W. 2001, MNRAS, 328, 393
 Ballard, K. R., & Heavens, A. F. 1992, MNRAS, 259, 89
 Bednarz, J., & Ostrowski, M. 1998, Phys. Rev. Lett., 80, 3911.
 Bell, A. R. 1978, MNRAS, 182, 147.
 Blandford, R., & McKee, C. 1977, Phys. Fluids, 19, 1130.
 Casse, F., Lemoine, M., & Pelletier, G. 2001, Phys. Rev. D, 65, 023002.
 Ellison, D., & Double, G. 2002, Astroparticle Physics, 18, 213.
 Gallant, Y. A., & Achterberg, A. 1999, MNRAS, 305, L6.
 Gallant, Y. A. et al. 2000, in Gamma-Ray Bursts, eds. R. M. Kippen et al., AIP Conference Series, Vol.526, p.524 (New-York: American Institute of Physics)
 Gallant, Y. A. 2002, to appear in Relativistic Flows in Astrophysics, eds. A. W. Guthmann et al., Lecture Notes in Physics (Berlin: Springer-Verlag), arXiv:astro-ph/0201243
 Gialis, D. & Pelletier, G., Astropart. Phys. in press, arXiv:astro-ph/0302231.
 Kirk, J. G., & Schneider, P. 1987, ApJ, 315, 425
 Kirk, J., & Duffy, P. 1999, J. Phys. G, 25, R163.
 Kirk, J., Guthmann, A., Gallant, Y., & Achterberg, A. 2000, ApJ, 542, 235.
 Ostrowski, M. 1993, MNRAS, 264, 248
 Peacock, J. 1981, MNRAS, 196, 135.
 Vietri, M. 1995, ApJ, 453, 883.
 Vietri, M. 2002, arXiv:astro-ph/0212352.
 Waxman, E. 1995, Phys. Rev. Lett., 75, 386.